Redox Exchange Induced MnO_2 Nanoparticle Enrichment in Poly(3,4-ethylenedioxythiophene) Nanowires for Electrochemical Energy Storage

Ran Liu,[†] Jonathon Duay,[†] and Sang Bok Lee[†,‡,*]

[†]Department of Chemistry and Biochemistry, University of Maryland, College Park, Maryland 20742 and [‡]Graduate School of Nanoscience and Technology (WCU), Korea Advance Institute of Science and Technology, Daejeon 305-701, Korea

ABSTRACT MnO_2 nanoparticle enriched poly(3,4-ethylenedioxythiophene) (PEDOT) nanowires are fabricated by simply soaking the PEDOT nanowires in potassium permanganate ($KMnO_4$) solution. The structures of these MnO_2 nanoparticle enriched PEDOT nanowires are characterized by SEM and TEM, which show that the MnO_2 nanoparticles have uniform sizes and are finely dispersed in the PEDOT matrix. The chemical constituents and bonding of these composite nanowires are characterized by energy-dispersive X-ray analysis, X-ray photoelectron spectroscopy, and infrared spectroscopy, which indicate that the formation and dispersion of these MnO_2 nanoparticles into the nanoscale pores of the PEDOT nanowires are most likely triggered by the reduction of $KMnO_4$ *via* the redox exchange of permanganate ions with the functional group on PEDOT. Varying the concentrations of $KMnO_4$ and the reaction time controls the loading amount and size of the MnO_2 nanoparticles. Cyclic voltammetry and galvanostatic charge—discharge are used to characterize the electrochemical properties of these MnO_2 nanoparticle loaded PEDOT nanowires. Due to their extremely high exposed surface area with nanosizes, the pristine MnO_2 nanoparticles in these MnO_2 nanoparticle enriched PEDOT nanowires show very high specific capacitance (410 F/g) as the supercapacitor electrode materials as well as high Li^+ storage capacity (300 mAh/g) as cathode materials of Li ion battery, which boost the energy storage capacity of PEDOT nanowires to 4 times without causing excessive volume expansion in the polymer. The highly conductive and porous PEDOT matrix facilitates fast charge/discharge of the MnO_2 nanoparticles and prevents them from agglomerating. These synergic properties enable the MnO_2 nanoparticle enriched PEDOT nanowires to be promising electrode materials for supercapacitors and lithium ion batteries.

KEYWORDS: heterostructured nanomaterials · nanowire · manganese oxide · PEDOT · electrochemical energy storage · supercapacitor · lithium ion battery

Heterostructured nanomaterials, such as coaxial nanowires, core—shell nanoparticles, and nanostructured composites, are drawing a tremendous amount of attention in the nanoscience research field because they offer not only extraordinary properties brought about by confining their dimensions but also synergic properties or functionalities from combining different materials.[1−11] There are a variety of ways to assemble nanocomponents into heterostructured nanomaterials. For example, layer-by-layer (LBL) assembly[4,12,13] has been widely used to fabricate core—shell nanoparticle[4] and coaxial nanowires.[6,13] They form by coating two or more layers of different materials onto existing nanostructured materials. A straightforward and powerful method for fabricating nanostructured composites is to disperse or assemble inorganic nanoparticles (*e.g.*, metal[14−16] and magnetic nanocystals[17]) with small sizes into the matrices, voids, and pores, or surfaces of nanostructured hosting materials[18] (*e.g.*, polymer nanowires,[8,14] silica nanotubes,[17] or TiO_2 nanotubes[16]).

To date, heterostructured nanomaterials with metal oxide and conductive polymer have been rarely reported.[19,20] In our previous paper, we reported the synthesis of coaxial MnO_2/poly(3,4-ethylenedioxythiophene) (PEDOT) nanowires by a one-step coelectrodeposition method.[21] Herein, we report the loading of finely dispersed MnO_2 nanoparticles into PEDOT nanowires by simply soaking PEDOT nanowires into a potassium permanganate solution. We describe the synthesis of the nanowires and nanoparticles, characterize their chemical constituents and bonding, propose a mechanism of MnO_2 formation, and report the electrochemical energy storage properties and volume change of the nanostructures. The pristine MnO_2 nanoparticles in these MnO_2 nanoparticle enriched PEDOT nanowires show very high specific capacitance (410 F/g) as supercapacitor electrode materials due to their extremely high exposed surface area with nanosizes. By the same token, these nanoparticles almost reach the theoretical limit of Li^+ insertion

*Address correspondence to slee@umd.edu.

Received for review May 10, 2010 and accepted June 22, 2010.

Published online June 30, 2010.
10.1021/nn1010182

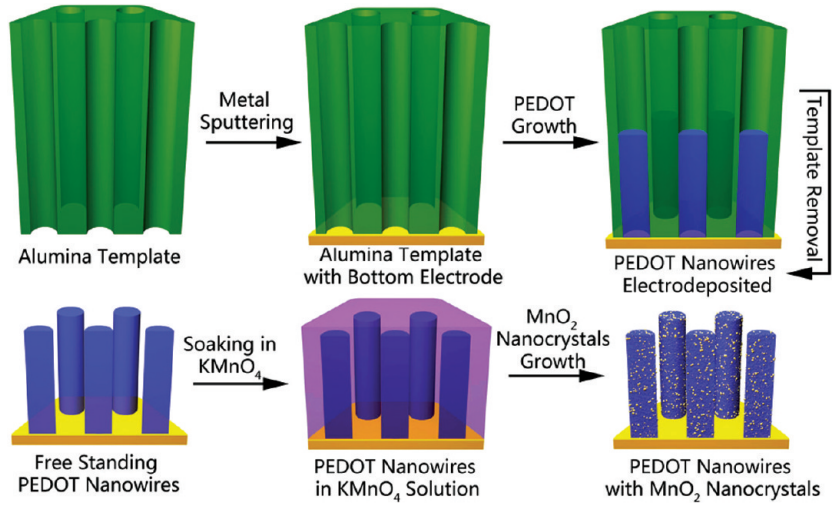

Scheme 1. Synthesis of MnO_2-NP/PEDOT composite nanowires.

coefficient and charge storage capacity as the potential cathode materials in the Li ion battery.

One advantage of this synthetic method is that no additional steps are needed to prepare MnO_2 nanoparticles before synthesizing the heterostructured material. When the PEDOT nanowires enter the solution, $KMnO_4$ is reduced *via* the redox exchange of permanganate ions with the functional group on PEDOT, triggering the formation and simultaneous spread of MnO_2 nanoparticles into the nanoscale pores of the nanowires. Varying the concentrations of $KMnO_4$ and the reaction time controls the loading amount and size of the MnO_2 nanoparticles.

Compared to the heterostructured MnO_2/PEDOT coaxial nanowires in our previous report,[21] MnO_2 and PEDOT are more uniformly mixed in the heterostructured nanowires. As mentioned earlier, these imbedded MnO_2 nanoparticles have ultrahigh surface area, which enhance the energy storage capacity of PEDOT (*e.g.*, to a high specific capacitance of 252 F/g) but without causing excessive volume expansion in the polymer. The highly conductive and porous PEDOT matrix facilitates fast charge/discharge of the MnO_2 nanoparticles and prevents them from agglomerating. These combined properties enable the MnO_2 nanoparticle enriched PEDOT nanowires, when applied as the electrode materials for supercapacitors, to have well-maintained high specific capacitance even at high charge/discharge rates.

RESULTS AND DISCUSSION

Scheme 1 illustrates the synthesis of MnO_2 nanoparticle loaded PEDOT nanowires, which will be abbreviated as MnO_2-NP/PEDOT nanowires. PEDOT nanowires were first electrodeposited in an alumina template and then exposed by template removal. The freestanding PEDOT nanowires were subsequently soaked in potassium permanganate solution for various times. MnO_2 nanoparticles grew in the PEDOT matrix during this soaking process.

The color of the PEDOT nanowires turned from navy blue (Figure 1a) to a green hue (Figure 1b) when the brownish colored MnO_2 NP formed. It is worth noting that the thus-formed MnO_2 nanoparticles can be

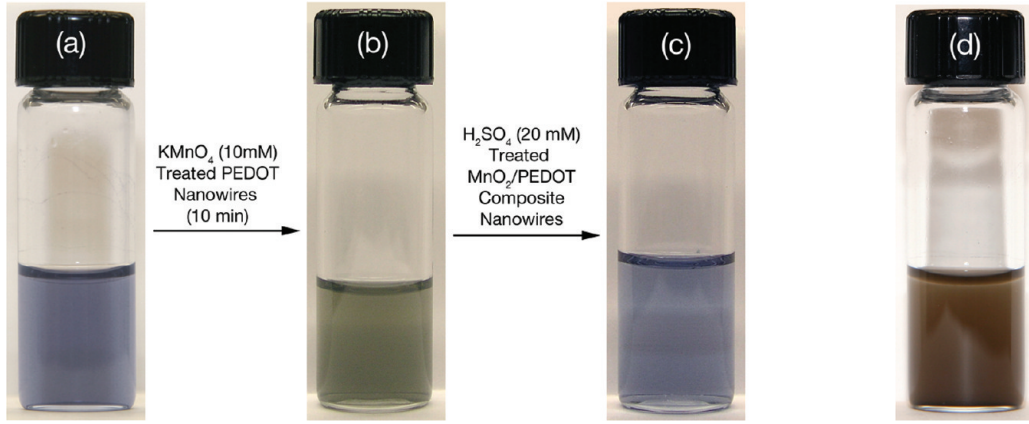

Figure 1. Digital images of (a) PEDOT nanowires dispersed in ethanol, (b) MnO_2-NP/PEDOT nanowires in ethanol. (c) Sulfuric acid treated MnO_2-NP/PEDOT nanowires, MnO_2 is stripped off (d) overoxidized PEDOT nanowires after soaking PEDOT nanowires in 10 mM $KMnO_4$ for 30 min.

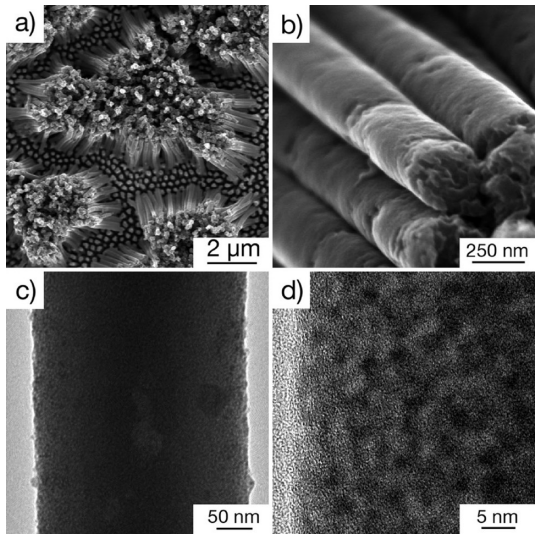

Figure 2. (a,b) SEM and (c,d) TEM images at different magnifications of PEDOT nanowires after being treated with $KMnO_4$ (10 mM) for 10 min.

stripped off by dilute sulfuric acid, which causes the PEDOT nanowires to return to navy blue color (Figure 1c). Soaking the nanowires in higher concentrations of $KMnO_4$ or at longer times will etch and overoxidize the PEDOT matrix (discussed later), rendering the PEDOT nanowires brownish in color, as shown in Figure 1d.

The SEM image (Figure 2a) of the $KMnO_4$ treated PEDOT nanowires shows that they aggregated into piles driven by surface tension during solvent evaporation. To prevent aggregation from affecting the electrochemical testing, the electrode never was allowed to completely dry. Figure 2b shows the high resolution SEM image of the same nanowires, which reveals their cigar shapes and rough surfaces. Figure 2c is the TEM image from a segment of $KMnO_4$ treated PEDOT nanowire. Some dark nanoparticles are vaguely visible but are clearer in a higher resolution TEM image (Figure 2d). These nanoparticles are less than 5 nm in size and finely dispersed in the PEDOT matrix. XRD studies show that the nanoparticles are X-ray amorphous, but TEM studies show that the nanoparticles have weak crystalline structures, which may have formed due to annealing caused by the TEM electron beams. The lattice spaces and electron diffraction ring patterns only partially match the XRD indices of α-MnO_2. (See Supporting Information SI1.) Thus these embedded MnO_2 nanoparticles are probably in the forms of amorphous MnO_2 or weakly crystallized α-MnO_2, which has been studied for its application in the electrode materials of supercapacitors.[22,23]

Additional methods were used to analyze the $KMnO_4$ treated nanowire and confirm the existence of MnO_2. Figure 3a−d shows the TEM images, Mn K map, S (sulfur from the thiophene ring on PEDOT) K map, and their mixed map on a segment of MnO_2-NP/PEDOT nanowire. Figure 3e shows the EDS spectra from a single MnO_2-NP/PEDOT nanowire. The atomic ratio of Mn to S in the nanowire is 1.42:1, which suggests that a large amount of MnO_2 NP has been loaded into the PEDOT matrix.

Figure 4 shows the XPS spectra obtained from the MnO_2 NP loaded PEDOT nanowires. The peaks of Mn $2p_{3/2}$ and Mn $2p_{1/2}$, which are centered at 642 and 653.8 eV, respectively, with a spin energy separation of 11.8 eV, are in good agreement with reported data of Mn $2p_{3/2}$ and Mn $2p_{1/2}$ in MnO_2.[24]

We propose and discuss several plausible mechanisms of MnO_2 formation. On the basis of the Mn/S ratio shown in Figure 3e, we can assume that 1 mol of PEDOT can encapsulate *ca.* 1.4 mol of MnO_2 NP. This process requires 4.2 mol of electrons to reduce the 1.4 mol of $KMnO_4$. However, it is difficult to conceive that 1 mol of PEDOT can provide 4.2 mol of electrons because the PEDOT is the already oxidized form of EDOT. The maximum number of electrons it can provide depends on its doping level, which is 0.3.[25] This suggests that 1 mol of PEDOT can only provide 0.3 mol of delocalized electrons during the doping (oxidation) process, which is not enough to reduce 1.4 mol of $KMnO_4$.

By looking at the structure of PEDOT, one would find that there are unsaturated bonds on the PEDOT conjugated rings, which might be broken and oxidized by the $KMnO_4$. If breakage occurs, the oxidation will destroy the conjugation of PEDOT, and it will lose its conductivity and electroactivity. However, experimental tests ruled out this possibility: After the MnO_2 NPs are loaded in the PEDOT matrix, dilute sulfuric acid was applied to the heterostructured nanowires to strip off the MnO_2. Electrochemical tests on these MnO_2 stripped PEDOT nanowires showed that the electrochemical properties were retained (data not shown) when compared to the electrochemical properties of PEDOT nanowires before MnO_2 NP insertion.

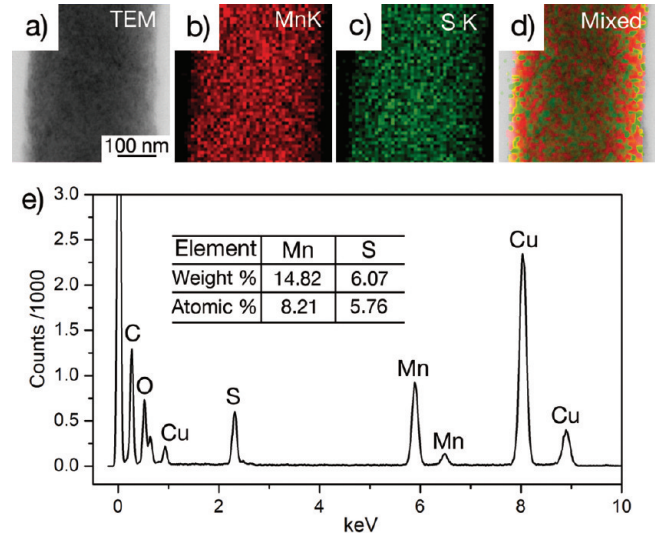

Figure 3. (a) TEM image and EDS mapping of (b) Mn, (c) S, and (d) mixture of Mn and S on a segment of MnO_2-NP/PEDOT nanowires.

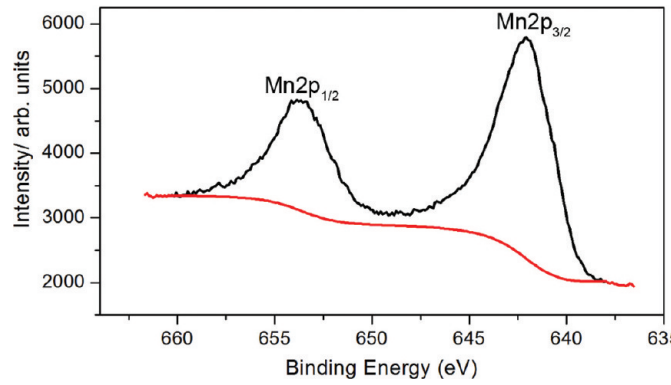

Figure 4. XPS spectra for manganese in the $KMnO_4$ treated PEDOT nanowires.

On the basis of the above analysis, the mechanism of MnO_2 NP formation becomes more ambiguous. Taking a glance at the EDOT monomer structure, however, reveals another possibility: The sulfur on the thiophene ring may serve as a site for $KMnO_4$ reduction. Indeed, MnO_2 nanoparticles have been synthesized previously by reducing $KMnO_4$ at the nitrogen sites of aniline monomers.[26]

Figure 5a shows the IR spectra of PEDOT nanowires treated with different concentration of $KMnO_4$ for 10 min. An absorbance peak at 1044 cm^{-1} gradually appears as the concentration of $KMnO_4$ increases and can be identified clearly when the $KMnO_4$ concentration reaches 50 mM. The arising peak at 1044 cm^{-1} can be assigned to the sulfoxide (S═O bond) stretching mode,[27] which suggests possible oxidation of the thiophene sulfur into sulfoxide by $KMnO_4$ (see Scheme 2.) Figure 5b shows that the sulfur peak shifts slightly to the higher binding energy after the PEDOT has been treated by $KMnO_4$, which suggests that the sulfur has been oxidized. The new peak (168 eV) in XPS analysis alludes to the possible oxidation of thiophene sulfur into the sulfone O═S═O group.[28] Similar oxidation on the sulfur sites of PEDOT:PSS by hydrogen peroxide[29] or NaOCl[30] has been described elsewhere. Oxidation of sulfides to corresponding sulfones by $KMnO_4$ is also reported.[31] In order to prevent PEDOT from losing its electroactivity, the concentration of $KMnO_4$ and the soaking time were kept low and short so that only a small portion of the PEDOT is oxidized. It is worth noting that only partial oxidation of thiophene sulfur sites on PEDOT will not be able to provide enough electrons

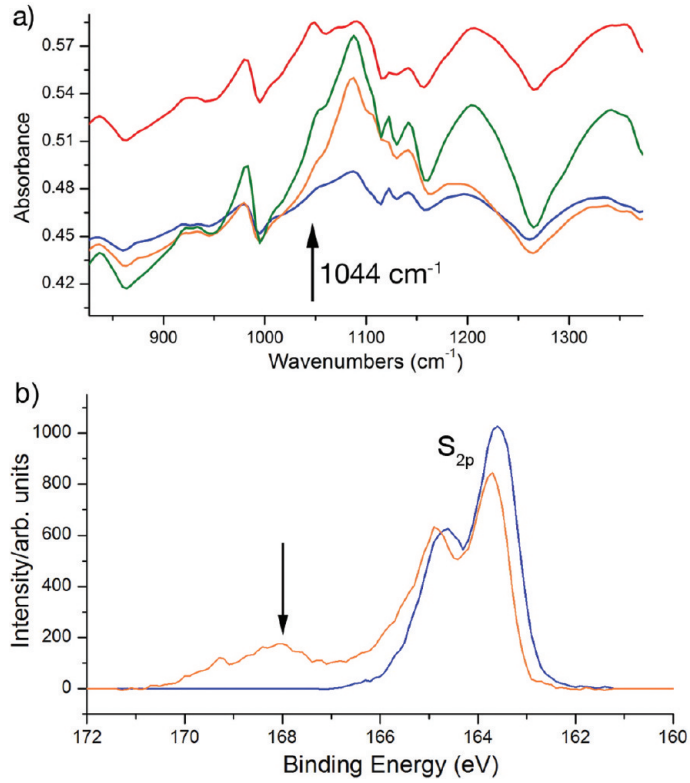

Figure 5. (a) IR spectra of PEDOT nanowire (blue) and PEDOT nanowires treated with 10 mM (orange), 20 mM (green), and 50 mM (red) $KMnO_4$ for 10 min. (b) XPS spectra of PEDOT before (blue) and after (orange) treatment with $KMnO_4$.

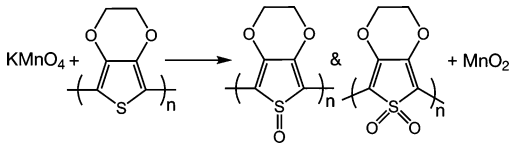

Scheme 2. Reduction of $KMnO_4$ by PEDOT to form MnO_2.

for the $KMnO_4$ reduction ratio of 1.4:1 MnO_2/PEDOT. Nevertheless, such reduction reactions may form the initial seeds that accelerate the water reduction of $KMnO_4$ to MnO_2 and further grow the MnO_2 nanoparticles.

We also analyzed the effects of the soaking conditions on the Mn/S ratio in the PEDOT nanowires. By controlling the soaking time and the concentration of the $KMnO_4$, we can regulate the loading amount of MnO_2. Figure 6a shows the Mn/S ratio in the nanowires as determined by EDS analysis after PEDOT reacted with different concentrations of $KMnO_4$ for 1 min. It is worth noting that the MnO_2 loading increases more rapidly at higher concentration of $KMnO_4$, which could be caused by the complete etching away of PEDOT after it is overoxidized into soluble product.[29,30] Figure 6b shows how the Mn/S ratio responds to the soaking time more linearly.

It is interesting to note that not only can the loading amount of MnO_2 be varied but also the nanoparticle size and structure can be tuned when different concentrations of $KMnO_4$ or different soaking times are applied (see Supporting Information SI2).

In order to study the electrochemical energy storage benefits of loading MnO_2 into the PEDOT matrix, cyclic voltammetry (CV) (Figure 7a and Supporting Information SI3) and galvanostatic charge/discharge (Figure 7b and Supporting Information SI4) tests were performed on the PEDOT nanowires before and after $KMnO_4$ treatment. As we can see from Figure 7a, CV shapes of PEDOT nanowires before and after MnO_2 NP enrichment all look like a rectangular envelope, which suggests that both PEDOT nanowires and MnO_2-NP/PEDOT nanowires have good capacitive properties at this scan rate. The inclusion of MnO_2 nanoparticles has resulted in the capacitive current increasing 4-fold. Both techniques are used to calculate the specific capacitances of MnO_2-NP/PEDOT nanowires at various current densities (see Supporting Information SI5). Thus, the calculated specific capacitance of MnO_2-NP/PEDOT nanowires is 250 F/g, which is higher than our previously reported MnO_2/PEDOT coaxial nanowires.[21] Eighty percent of the maximum specific capacitance is maintained, while the current density is boosted over 25 mA/cm^2 (see Supporting Information SI6). The well-maintained capacitance value even at high current density or high charge/discharge rate is due to small dimensions of the PEDOT nanowires and MnO_2 NPs as well as as the high conductivity of PEDOT.[21,32,33] Due to the large specific surface area of MnO_2 NPs, the pristine specific capacitance of MnO_2 NPs can be calculated as 410 F/g, which is higher than other synthesized nanostructured MnO_2 supercapacitor electrodes at the same charge/discharge rate[26,34−36] (see Supporting Information SI5). Figure 7b also demonstrates that the MnO_2-NP/PEDOT nanowires can serve as potential cathode materials for lithium ion battery. It shows that the charge capacity significantly increased at least 4 times after loading of MnO_2 nanoparticles. Indeed, nanostructured MnO_2 or PEDOT has been reported for applications in lithium ion batteries.[24,37−39] The pristine charge storage capacity of MnO_2 can be estimated as 300 mAh/g, which is very close to the theoretical charge storage capacity of MnO_2 (308 mAh/g). The corresponding lithium insertion coefficient (x value in the Li_xMnO_2) can be calculated as 0.97, which is also very close to the maximum value of 1. Such high insertion coefficient is due to complete lithium intercalation into the small nanosized MnO_2 nanoparticles (see Supporting Information SI5).

The electrochemical stability test of the MnO_2 NP enriched PEDOT nanowires was performed using cycled galvanostatic charge/discharge methods. As shown in Figure 8, the MnO_2-NP/PEDOT nanowires displayed satisfactory electrochemical stability. On the basis of the charge/discharge time, the charge storage capacity loss can be calculated as 10% loss after 500 cycles and 2% loss after 100 cycles. In addition, the charge/discharge

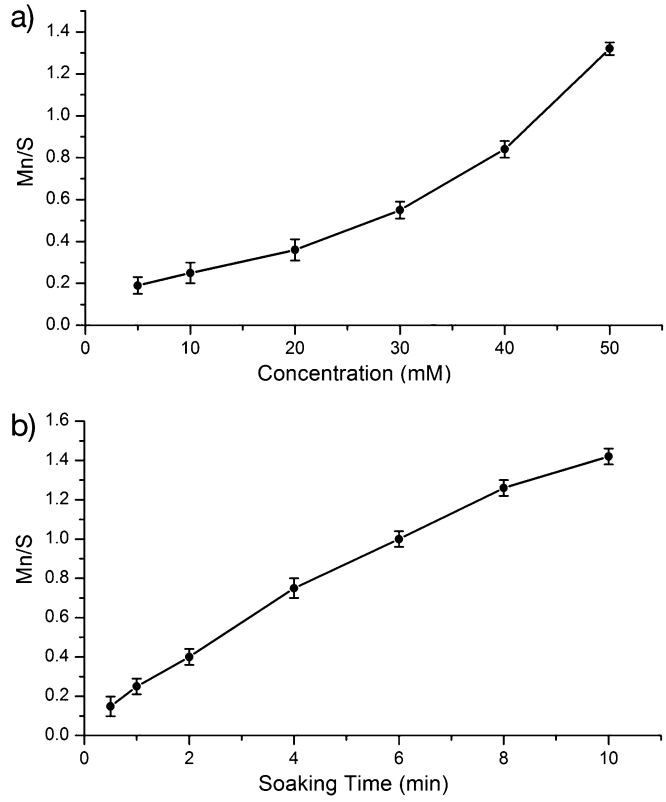

Figure 6. MnO_2 loading capacity (Mn/S ratio) *versus* (a) different concentrations of $KMnO_4$ for 1 min and (b) different soaking times in 10 mM $KMnO_4$.

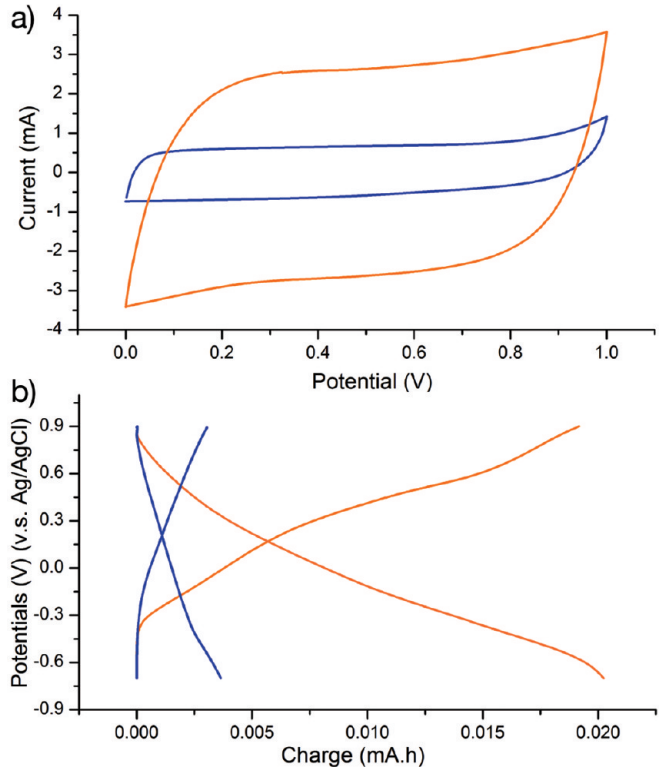

Figure 7. (a) Cyclic voltammograms of PEDOT nanowires before (blue) and after (orange) 10 mM $KMnO_4$ treatment (10 min) scanned at 100 mV/s between 0 and 1 V in 1 M $LiClO_4$ in water. (b) Galvanostatic charge/discharge curves of PEDOT nanowires (blue) and MnO_2-NP/PEDOT nanowires (orange) at current density of 1.25 mA/cm^2 in 1 M $LiClO_4$ in propylene carbonate, which corresponds to the 10 C high charge/discharge rate.

curve maintained symmetrical shapes after 100 and 500 cycle tests.

It is worth noting that, although the inclusion of MnO_2 NPs significantly increases the charge capacity of PEDOT nanowires, the volume of the PEDOT did not expand significantly. Figure 9 shows the TEM images of PEDOT nanowires (grown on Au substrate) before and after the $KMnO_4$ treatment. The d_{PEDOT} and $d_{MnO_2/PEDOT}$ represent the diameters of the PEDOT nanowire

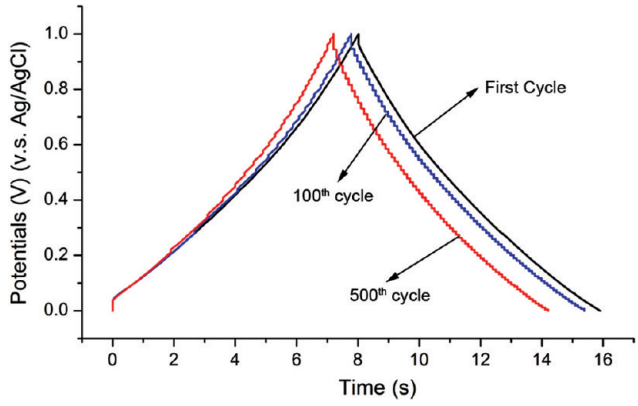

Figure 8. Electrochemical stability for the MnO_2 NP enriched PEDOT nanowires. Galvanostatic charge/discharge tests are performed between 0 and 1 V (*vs* Ag/AgCl) at current density of 30 mA/cm^2 on the MnO_2 NP enriched PEDOT nanowires in 1 M $LiClO_4$ solution for 500 cycles.

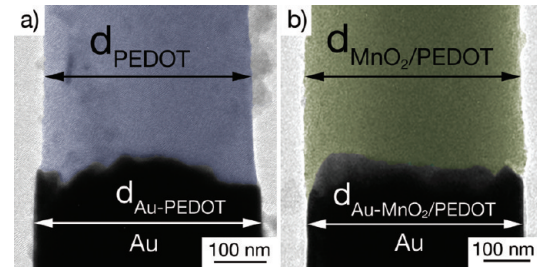

Figure 9. Volume expansion of PEDOT nanowires before and after loading MnO_2 NP (PEDOT nanowires are treated in 10 mM $KMnO_4$ for 10 min).

before and after $KMnO_4$ treatment, and $d_{Au/PEDOT}$ and $d_{Au\text{-}MnO_2/PEDOT}$ represent the diameters of the their corresponding gold bottom. The diameter expansion of the MnO_2-NP/PEDOT nanowires is less than 8%, which is easily accommodated by the available space between the PEDOT nanowires after template removal.

Assuming that the diameter of the bottom gold is not affected by the $KMnO_4$, and the PEDOT nanowire swelling is isotropic, the volume expansion rate is

$$\frac{V_2 - V_1}{V_1} = \left(\frac{d_{MnO_2/PEDOT}/d_{Au\text{-}MnO_2/PEDOT}}{d_{PEDOT}/d_{Au\text{-}PEDOT}} - 1 \right)^3 \quad (1)$$

where d_{PEDOT} and $d_{MnO_2/PEDOT}$ represent the diameters of the PEDOT nanowire before and after $KMnO_4$ treatment and $d_{Au/PEDOT}$ and $d_{Au\text{-}MnO_2/PEDOT}$ represent diameters of the their corresponding gold bottom. The calculated volume expansion is 25%.

Volume expansion of the PEDOT nanowire can also be theoretically estimated by the equation

$$\frac{V_2 - V_1}{V_1} = \frac{n_2}{n_1}\frac{d_1 M_2}{d_2 M_1} \quad (2)$$

where n_2/n_1 is the mole ratio of the MnO_2 to PEDOT (herein 1.42), d_2 and d_1 are the densities of MnO_2 and PEDOT,[40] and M_2 and M_1 are the molecular weights of MnO_2 and PEDOT. On the basis of eq 2, the estimate of the volume expansion is 28%, which well matches the experimentally obtained volume expansion. The small volume expansion is mainly due to the low volumetric mass density and high porosity of the PEDOT matrix, which provides spaces to include a large amount of MnO_2.

In our previous paper,[21] for the MnO_2/PEDOT coaxial nanowires synthesized at 0.75 V, the core MnO_2 takes 25% of the total volume, and the mole ratio of Mn to S is approximately 1:1. In this paper, for the MnO_2-NP/PEDOT nanowires, the MnO_2 nanoparticles take 20% of the total volume while maintaining the mole ratio of Mn to S at 1.42:1. Such high loading capacity is probably because the chemically formed MnO_2 nanoparticles are denser than the electrodeposited nanostructures. Thus, incorporated MnO_2nanoparticles utilize less space while providing more energy capac-

ity, which further increases the energy density and power density per volume.

CONCLUSION

In summary, we described the fabrication of MnO_2 nanoparticle loaded PEDOT nanowires by simply soaking the PEDOT nanowires in $KMnO_4$ solution. On the basis of the spectroscopic evidence from IR and XPS for the S═O group formation in the PEDOT, the formation of MnO_2 nanoparticles is most likely triggered by the redox exchange of $KMnO_4$ with the sulfur sites on the PEDOT structures. The nanosized MnO_2 nanoparticles can efficiently store the lithium ions and boost the energy storage capacity by 4 times. The hosting material, highly conductive and porous PEDOT, facilitates the fast charge/discharge rate of the MnO_2 nanoparticles and prevents them from aggregating. These synergic properties enable the MnO_2 NP enriched PEDOT nanowires to be promising electrode materials with high capacitance at high charge/discharge rates for supercapacitors and lithium ion batteries. The present work may pave a new pathway of controlled synthesis of other inorganic/organic multifunctional heterostructured nanomaterials *via* chemical reaction of oxidative inorganic precursor and polymer materials with a reductive functional group.

METHODS

Chemicals and Materials. 3,4-Ethylenedioxythiophene (EDOT) was obtained from Aldrich (Milwaukee, WI). Lithium perchlorate and potassium permanganate were obtained from Fisher Scientific (FairLawn, NJ). Acetonitrile and propylene carbonate were obtained from Sigma Aldrich. Gold electroplating solution (Orotemp 24) was purchased from Technic (Cranston, RI). Deionized water (*ca.* 18/MΩ · cm resistivity) was obtained by using a Milli-Q water purification system from Millipore (Dubuque, IA). Alumina membranes, with a pore diameter of 200 nm and thickness of 60 μm, are commercially available from Whatman (Clifton, NJ).

Synthesis. PEDOT nanowires were synthesized potentiostatically (1.2 V) in the acetonitrile solution of 100 mM EDOT and 100 mM $LiClO_4$. All potentials were measured relative to a Ag/AgCl reference electrode using a Pt foil as a counter electrode, if not specified otherwise. Alumina template was subsequently removed by 3 M NaOH solution to expose the PEDOT nanowires. MnO_2 nanoparticles were loaded into the PEDOT nanowires by soaking the above exposed PEDOT nanowires in potassium permanganate solution with different concentrations (5−50 mM), depending on the desired amount of MnO_2 nanoparticles to be loaded. $KMnO_4$ (especially under acidic environment) is a very powerful oxidizing reagent, which may overoxidize the PEDOT. To prevent this overoxidization, we use neutral $KMnO_4$ solution with low concentration (typical 10 mM) and short treating time (typical 10 min). Gold bottoms for the volume expansion studies were electrochemically deposited at the current density of −1 mA/cm^2 for 30 min in the Orotemp 24 gold plating solution. The preparation of a working electrode is as follows: First, a thin layer of gold (*ca.* 500 nm) was sputtered onto the branched side of an alumina membrane with a Denton Vacuum Desktop III sputtering system. The Au-coated membrane was connected to an electrical circuit using a copper tape (3M). Defining and sealing an electroactive window (0.32 cm^2 in nominal area) was performed using silicone rubber or parafilm. Considering the porosity of the membrane (60%), the corrected surface area of the electroactive window was 0.2 cm^2. The mass and the length (thickness in film) of the resulting PEDOT nanowires were controlled by fixing the total charges passed during the electrodeposition. Typically, coaxial nanowires with lengths of 10 μm can be obtained after the charge passed about 200 mC. Diameters of these nanowires correspond to the pore diameters of the alumina template (*ca.* 300 nm).

Characterization. The MnO_2-NP/PEDOT nanowires were investigated using a field emission scanning electron microscope (Hitachi SU-70 SEM, operated at an acceleration voltage of 10 keV) and transmission electron microscope (JEOL JEM 2100 field emission transmission electron microscope (FE-TEM), 200 keV). The sampling methods for SEM and TEM analysis are briefly described: gold-coated side of a small piece of an alumina template was tightly attached onto an SEM specimen holder by using a carbon tape. The template was dissolved to expose the nanowires by using 3 M NaOH. After rinsing it with deionized water repeatedly, the sample was dried in air before observation. For TEM sampling, sonication is applied to the MnO_2-NP/PEDOT to disperse them in ethanol. The released nanowires were repeatedly rinsed with deionized water and ethanol. Then, 6 μL of the nanowire solution was dropped and dried on a TEM grid.

FT-IR spectra were obtained using a Thermo Nicolet Nexus 670 FT-IR instrument equipped with a photoelastic modulation module. The spectra were collected using a DTGS KBr detector. The samples were prepared by soaking electrodeposited PEDOT films in various concentrations of $KMnO_4$ (0, 10, 20, and 50 mM) for 10 min. The PEDOT and resulting MnO_2/PEDOT films were then ground with KBr and pressed into homogeneous pellets. Each pellet including a blank for the background was scanned 32 times from 4000 to 400 cm^{-1} using the FT-IR instrument with a resolution of 4 cm^{-1}. Background subtraction was done by Omnic software in auto gain mode.

XPS analysis was done on Kratos AXIS 165 spectrometer. C 1s (for hydrocarbon or hydrocarbon groups) = 284. Eight electronvolts was used as the calibrant.

The electrochemical studies of MnO_2-NP/PEDOT nanowires are performed in the standard three-electrode system; Ag/AgCl is used as the reference electrode, and Pt foil is used as the counter electrode. In order to calculate specific capacitance, cyclic voltammetry at different scan rates (100−500 mV/s) and galvanostatic charge/discharge tests at different current densities (10−50 mA/cm^2) were performed by cycling potential from 0 to 1 V in 1 M $LiClO_4$ in water. Aqueous system is chosen because the charge/discharge speed of MnO_2-NP/PEDOT will be faster in the water system, which is critical in the supercapacitor application. Galvanostatic charge/discharge for the lithium ion insertion study is done by cycling the potential from −0.7 to 0.9 V at current density of 1.25 mA/cm^2 (corresponds to about 10 C charge/discharge rate for MnO_2-NP/EPDOT nanowires) in the solution of 1 M $LiClO_4$ in the propylene carbonate. Organic solvent (PC) is chosen to achieve the broader range of electrochemical windows and prevent the electrolyte from drying. All of the above electrochemical experiments were performed using a bipotentiostat (BI-STAT; Princeton Applied Research).

Acknowledgment. The work was supported by the UMD-NSF-MRSEC under Grant DMR 05-20471, Laboratory for Physical Sciences, Nanoscale Imaging Spectroscopy and Properties (NISP) Laboratory, and also supported as part of the Science of Precision Multifunctional Nanostructures for Electrical Energy Storage, an Energy Frontier Research Centre funded by the U.S. Department of Energy, Office of Science, Office of Basic Energy Sciences under Award Number DESC0001160 (J.D. and S.B.L.). S.B.L. research was also supported by WCU program through the KOSEF funded by the MEST (Grant No. R31-2008-000-10071-0). We thank L. Lai (NISP Lab) and for assistance with SEM and TEM. We sincerely thank Dr. Ashley Predith for a useful discussion on this paper.

Supporting Information Available: High-resolution TEM and electron diffraction patterns of the MnO_2 nanoparticles. TEM images of MnO_2-NP/PEDOT nanowires with less $KMnO_4$ treating time. Cyclic voltammograms of MnO_2-NP/PEDOT nanowires at different scan rate. Galvanostatic charge/discharge curves of MnO_2-NP/PEDOT nanowires. Detailed calculations of specific capacitance, lithium storage capacity of the MnO_2-NP/PEDOT nanowires, and pristine MnO_2 nanoparticles. Specific capacitance of MnO_2-NP/PEDOT nanowires at different charge/discharge current densities. This material is available free of charge *via* the Internet at http://pubs.acs.org.

REFERENCES AND NOTES

1. Tian, B. Z.; Zheng, X. L.; Kempa, T. J.; Fang, Y.; Yu, N. F.; Yu, G. H.; Huang, J. L.; Lieber, C. M. Coaxial Silicon Nanowires as Solar Cells and Nanoelectronic Power Sources. *Nature* **2007**, *449*, 885–890.
2. Meduri, P.; Pendyala, C.; Kumar, V.; Sumanasekera, G. U.; Sunkara, M. K. Hybrid Tin Oxide Nanowires as Stable and High Capacity Anodes for Li-Ion Batteries. *Nano Lett.* **2009**, *9*, 612–616.
3. Chen, X.; Knez, M.; Berger, A.; Nielsch, K.; Gösele, U.; Steinhart, M. Formation of Titania/Silica Hybrid Nanowires Containing Linear Mesocage Arrays by Evaporation-Induced Block-Copolymer Self-Assembly and Atomic Layer Deposition. *Angew. Chem., Int. Ed.* **2007**, *46*, 6829–6832.
4. Kim, J. S.; Rieter, W. J.; Taylor, K. M. L.; An, H.; Lin, W. L.; Lin, W. B. Self-Assembled Hybrid Nanoparticles for Cancer-Specific Multimodal Imaging. *J. Am. Chem. Soc.* **2007**, *129*, 8962–8963.
5. Sides, C. R.; Croce, F.; Young, V. Y.; Martin, C. R.; Scrosati, B. A High-Rate, Nanocomposite $LiFePO_4$/Carbon Cathode. *Electrochem. Solid State* **2005**, *8*, A484–A487.
6. Taberna, L.; Mitra, S.; Poizot, P.; Simon, P.; Tarascon, J. M. High Rate Capabilities Fe_3O_4-Based Cu Nano-Architectured Electrodes for Lithium-Ion Battery Applications. *Nat. Mater.* **2006**, *5*, 567–573.
7. Katz, E.; Willner, I. Integrated Nanoparticle−Biomolecule Hybrid Systems: Synthesis, Properties, and Applications. *Angew. Chem., Int. Ed.* **2004**, *43*, 6042–6108.
8. Liu, R.; Duay, J.; Lane, T.; Lee, S. B. Synthesis and Characterization of RuO_2/Poly(3,4-ethylenedioxythiophene) Composite Nanotubes for Supercapacitors. *Phys. Chem. Chem. Phys.* **2010**, *12*, 4309–4316.
9. Kovtyukhova, N. L.; Mallouk, T. E. Nanowire P−N Heterojunction Diodes Made by Templated Assembly of Multilayer Carbon-Nanotube/Polymer/Semiconductor-Particle Shells around Metal Nanowires. *Adv. Mater.* **2005**, *17*, 187–192.
10. Alayoglu, S.; Nilekar, A. U.; Mavrikakis, M.; Eichhorn, B. Ru−Pt Core−Shell Nanoparticles for Preferential Oxidation of Carbon Monoxide in Hydrogen. *Nat. Mater.* **2008**, *7*, 333–338.
11. Schmidt, D. J.; Cebeci, F. C.; Kalcioglu, Z. I.; Wyman, S. G.; Ortiz, C.; Van Vliet, K. J.; Hammond, P. T. Electrochemically Controlled Swelling and Mechanical Properties of a Polymer Nanocomposite. *ACS Nano* **2009**, *3*, 2207–2216.
12. Srivastava, S.; Kotov, N. A. Composite Layer-by-Layer (LbL) Assembly with Inorganic Nanoparticles and Nanowires. *Acc. Chem. Res.* **2008**, *41*, 1831–1841.
13. Lauhon, L. J.; Gudiksen, M. S.; Wang, C. L.; Lieber, C. M. Epitaxial Core−Shell and Core−Multishell Nanowire Heterostructures. *Nature* **2002**, *420*, 57–61.
14. Guo, Y. G.; Hu, J. S.; Liang, H. P.; Wan, L. J.; Bai, C. L. Highly Dispersed Metal Nanoparticles in Porous Anodic Alumina Films Prepared by a Breathing Process of Polyacrylamide Hydrogel. *Chem. Mater.* **2003**, *15*, 4332–4336.
15. Sih, B. C.; Wolf, M. O. Metal Nanoparticle-Conjugated Polymer Nanocomposites. *Chem. Commun.* **2005**, 3375–3384.
16. Paramasivalm, I.; Macak, J. M.; Schmuki, P. Photocatalytic Activity of TiO_2-Nanotube Layers Loaded with Ag and Au Nanoparticles. *Electrochem. Commun.* **2008**, *10*, 71–75.
17. Son, S. J.; Reichel, J.; He, B.; Schuchman, M.; Lee, S. B. Magnetic Nanotubes for Magnetic-Field-Assisted Bioseparation, Biointeraction, and Drug Delivery. *J. Am. Chem. Soc.* **2005**, *127*, 7316–7317.
18. Gangopadhyay, R.; De, A. Conducting Polymer Nanocomposites: A Brief Overview. *Chem. Mater.* **2000**, *12*, 608–622.
19. Peng, X. S.; Jin, J.; Ichinose, I. Mesoporous Separation Membranes of Polymer-Coated Copper Hydroxide Nanostrands. *Adv. Funct. Mater.* **2007**, *17*, 1849–1855.
20. Nishizawa, M.; Mukai, K.; Kuwabata, S.; Martin, C. R.; Yoneyama, H. Template Synthesis of Polypyrrole-Coated Spinel $LiMn_2O_4$ Nanotubules and Their Properties as Cathode Active Materials for Lithium Batteries. *J. Electrochem. Soc.* **1997**, *144*, 1923–1927.
21. Liu, R.; Lee, S. B. MnO_2/Poly(3,4-ethylenedioxythiophene) Coaxial Nanowires by One-Step Coelectrodeposition for Electrochemical Energy Storage. *J. Am. Chem. Soc.* **2008**, *130*, 2942–2943.
22. Jiang, J. H.; Kucernak, A. Electrochemical Supercapacitor Material Based on Manganese Oxide: Preparation and Characterization. *Electrochim. Acta* **2002**, *47*, 2381–2386.
23. Toupin, M.; Brousse, T.; Bélanger, D. Influence of Microstucture on the Charge Storage Properties of Chemically Synthesized Manganese Dioxide. *Chem. Mater.* **2002**, *14*, 3946–3952.
24. Reddy, A. L. M.; Shaijumon, M. M.; Gowda, S. R.; Ajayan, P. M. Coaxial MnO_2/Carbon Nanotube Array Electrodes for High-Performance Lithium Batteries. *Nano Lett.* **2009**, *9*, 1002–1006.
25. Randriamahazaka, H.; Noël, V.; Chevrot, C. Nucleation and Growth of Poly(3,4-ethylenedioxythiophene) in Acetonitrile on Platinum under Potentiostatic Conditions. *J. Electroanal. Chem.* **1999**, *476*, 183.
26. Ragupathy, P.; Vasan, H. N.; Munichandraiah, N. Synthesis and Characterization of Nano-MnO_2 for Electrochemical Supercapacitor Studies. *J. Electrochem. Soc.* **2008**, *155*, A34–A40.
27. Fawcett, W. R.; Kloss, A. A. Solvent-Induced Frequency Shifts in the Infrared Spectrum of Dimethyl Sulfoxide in Organic Solvents. *J. Phys. Chem.* **1996**, *100*, 2019–2024.
28. Gardella, J. A.; Ferguson, S. A.; Chin, R. L. Π^*-Π Shakeup Satellites for the Analysis of Structure and Bonding in Aromatic Polymers by X-ray Photoelectron-Spectroscopy. *Appl. Spectrosc.* **1986**, *40*, 224–232.
29. Yoshioka, Y.; Calvert, P. D.; Jabbour, G. E. Simple Modification of Sheet Resistivity of Conducting Polymeric Anodes *via* Combinatorial Ink-Jet Printing Techniques. *Macromol. Rapid Commun.* **2005**, *26*, 238–246.
30. Yoshioka, Y.; Jabbour, G. E. Inkjet Printing of Oxidants for Patterning of Nanometer-Thick Conducting Polymer Electrodes. *Adv. Mater.* **2006**, *18*, 1307–1312.
31. Shaabani, A.; Mirzaei, P.; Naderi, S.; Lee, D. G. Green Oxidations. The Use of Potassium Permanganate Supported on Manganese Dioxide. *Tetrahedron* **2004**, *60*, 11415–11420.
32. Hu, C. C.; Chang, K. H.; Lin, M. C.; Wu, Y. T. Design and Tailoring of the Nanotubular Arrayed Architecture of Hydrous RuO_2 for Next Generation Supercapacitors. *Nano Lett.* **2006**, *6*, 2690–2695.
33. Liu, R.; Cho, S. I.; Lee, S. B. Poly(3,4-ethylenedioxythiophene) Nanotubes as Electrode Materials for a High-Powered Supercapacitor. *Nanotechnology* **2008**, *19*, 215710.
34. Wang, X. Y.; Wang, X. Y.; Huang, W. G.; Sebastian, P. J.; Gamboa, S. Sol−Gel Template Synthesis of Highly Ordered MnO_2 Nanowire Arrays. *J. Power Sources* **2005**, *140*, 211–215.
35. Shinomiya, T.; Gupta, V.; Miura, N. Effects of Electrochemical-Deposition Method and Microstructure on the Capacitive Characteristics of Nano-Sized Manganese Oxide. *Electrochim. Acta* **2005**, *51*, 4412–4419.
36. Wu, M. S. Electrochemical Capacitance from Manganese Oxide Nanowire Structure Synthesized by Cyclic Voltammetric Electrodeposition. *Appl. Phys. Lett.* **2005**, 87.

37. Liu, D. W.; Zhang, Q. F.; Xiao, P.; Garcia, B. B.; Guo, Q.; Champion, R.; Cao, G. Z. Hydrous Manganese Dioxide Nanowall Arrays Growth and Their Li^+ Ions Intercalation Electrochemical Properties. *Chem. Mater.* **2008**, *20*, 1376–1380.
38. Chen, J.; Liu, Y.; Minett, A. I.; Lynam, C.; Wang, J. Z.; Wallace, G. G. Flexible, Aligned Carbon Nanotube/Conducting Polymer Electrodes for a Lithium-Ion Battery. *Chem. Mater.* **2007**, *19*, 3595–3597.
39. Novák, P.; Müller, K.; Santhanam, K. S. V.; Haas, O. Electrochemically Active Polymers for Rechargeable Batteries. *Chem. Rev.* **1997**, *97*, 207–281.
40. Aasmundtveit, K. E.; Samuelsen, E. J.; Pettersson, L. A. A.; Inganäs, O.; Johansson, T.; Feidenhans, R. Structure of Thin Films of Poly(3,4-ethylenedioxythiophene). *Synth. Met.* **1999**, *101*, 561–564.